Ecotoxicology and Human Environmental Health

Structural features and pro-inflammatory effects of water-soluble organic matter in inhalable fine urban air particles

Antoine Simões Almeida, Rita Ferreira, Artur M. S. Silva, Armando C. Duarte, Bruno Neves, and Regina M.B.O. Duarte

Environ. Sci. Technol., **Just Accepted Manuscript** • DOI: 10.1021/acs.est.9b04596 • Publication Date (Web): 11 Nov 2019

Structural features and pro-inflammatory effects of water-soluble organic matter in inhalable fine urban air particles

Antoine S. Almeida,[1] Rita M. P. Ferreira,[2] Artur M. S. Silva,[2] Armando C. Duarte,[1] Bruno M. Neves,[3,§] Regina M. B. O. Duarte [1,§,]*

[1] Department of Chemistry & CESAM, University of Aveiro, 3810-193 Aveiro, Portugal

[2] Department of Chemistry & QOPNA and LAQV-REQUIMTE, University of Aveiro, 3810-193 Aveiro, Portugal

[3] Department of Medical Sciences and Institute of Biomedicine – iBiMED, University of Aveiro, 3810-193 Aveiro, Portugal

[§] *supervised this study equally as senior authors*

ABSTRACT

The impact of inhalable fine particulate matter ($PM_{2.5}$, aerodynamic diameter < 2.5 μm) on public health is of great concern worldwide. Knowledge on their harmful effects are mainly due to studies carried out with whole air particles, being the contribution of their different fractions largely unknown. Herein, a set of urban $PM_{2.5}$ samples were collected during day and nighttime periods in Autumn and Spring, aiming to address the seasonal and day-night variability of water-soluble organic matter (WSOM) composition. *In vitro* analysis of oxidative and pro-inflammatory potential of WSOM samples was carried out in both acute (24 h) and chronic (3 weeks) exposure setups using Raw264.7 macrophages as cell model. Findings revealed that the structural composition of WSOM samples differs between seasons and in a day-night cycle. Cells exposure resulted in an increase in the transcription of the cytoprotective *Hmox1* and pro-inflammatory genes *Il1b* and *Nos2*, leading to a moderate pro-inflammatory status. These macrophages showed an impaired capacity to subsequently respond to a strong pro-inflammatory stimulus such as bacterial lipopolysaccharide, which may implicate a compromised capacity to manage harmful pathogens. Further investigation on aerosol WSOM could help to constrain the mechanisms of WSOM-induced respiratory diseases and contribute to $PM_{2.5}$ regulations.

31

32

33

INTRODUCTION

Inhalable fine atmospheric particulate matter ($PM_{2.5}$, aerodynamic diameter < 2.5 μm) is of serious concerns in terms of health effects, including cardiovascular diseases,[1,2] airway damages and lung carcinogenesis,[2–4] and adverse neurodevelopmental effects.[5–7] Oxidative stress, genotoxicity, and inflammation have been suggested to be the central mechanisms by which $PM_{2.5}$ may impair the normal cellular physiological/biochemical processes, resulting in tissues damages and, therefore, facilitating the incidence and development of those adverse health outcomes.[2] Lung cells, such as epithelial cells and alveolar macrophages, are the primary targets of $PM_{2.5}$-induced oxidative damage and pro-inflammatory effects.[8–10] In the past, these effects have been linked to $PM_{2.5}$ mass concentration;[9,11] however, evidences indicate that $PM_{2.5}$ chemical composition play an important role in the interaction between fine particles and lung cells membrane.[10,12–17]

$PM_{2.5}$ is a complex mixture of inorganic and carbonaceous constituents, whose composition depends on the emission sources (natural and/or anthropogenic), formation process (*i.e.*, secondary origin), atmospheric processing, and weather conditions. A small set of chemical species have been linked to the oxidative potential and inflammatory

impact of ambient $PM_{2.5}$. These include water-soluble metals (*e.g.*, Fe, Ni, Cu, Cr, Mn, Zn, V, and Pb),[10,12,17,18] water-soluble ions (*e.g.*, SO_4^{2-}, NO_3^-),[10] solvent-extractable organic components, such as polycyclic aromatic hydrocarbons (PAHs) and PAH nitro-derivatives, polychlorinated biphenyls, organochlorine pesticides, and polybrominated diphenyl ethers,[16,18,19] and wood smoke tracers (*e.g.*, levoglucosan and galactosan).[19,20] Although not receiving much attention by the air pollution health research community, water-soluble organic matter (WSOM) of ambient $PM_{2.5}$ have been recently also recognized as capable of mediating reactive oxygen species (ROS) generation.[17,21–26] In Northern Hemisphere midlatitudes, this organic aerosol component represent 10 to 80% of the total particulate organics,[27–30] whereas lower percentage values (up to 13%) have been reported for Southern Hemisphere locations.[31] Based on highly informative off-line analytical techniques, such as multidimensional nuclear magnetic resonance (NMR) spectroscopy and high-resolution mass spectrometry, it has been shown that aerosol WSOM consists of a highly diverse suite of oxygenated compounds, including dicarboxylic acids, keto-carboxylic acids, aliphatic aldehydes and alcohols, saccharides, saccharide anhydrides, aromatic acids, phenols, but also amines, amino acids, organic

66 nitrates, and organic sulfates.[31–40] Although being a major fraction of organic aerosols,
67 the way by which the aerosol WSOM is redox-active or exert inflammation remains
68 unresolved. It contributes greatly to this situation the inherent complexity of aerosol
69 WSOM, with different chemical structures and associated physical properties. The use of
70 chemical assays, such as dithiothreitol (DTT), has suggested important contributions of
71 specific aerosol WSOM fractions, namely of isolated hydrophobic fractions (the so-called
72 "humic-like substances" operational concept),[21,22,25] on the oxidative potential of ambient
73 $PM_{2.5}$. However, no evidence exists on which structural components of aerosol WSOM
74 actually induce oxidative stress and inflammation. An enhanced knowledge of the relative
75 contribution of WSOM substructures to the oxidative and pro-inflammatory potential of
76 this organic aerosol fraction would be useful to understand the net impacts of air
77 particulate organic matter on human health.
78 Within this context, this study aims to establish a relationship between the oxidative and
79 pro-inflammatory potential of aerosol WSOM and their atmospheric concentrations and
80 structural characteristics. A set of $PM_{2.5}$ samples were collected at an urban location,
81 during day and nighttime periods, in Autumn and Spring seasons. With this $PM_{2.5}$

sampling scheme, it was intended to apportion the seasonal and day-night variability of WSOM structures to their oxidative and pro-inflammatory potential. The compositional features of aerosol WSOM samples were exploited by liquid-state one-dimensional (1D) and two-dimensional (2D) NMR spectroscopy. The effects of aerosol WSOM on nitric oxide (NO) production, ROS cellular levels, transcription of the inflammatory genes *Il1b* and *Nos2*, as well as activation of associated signalling pathway NF-κB were assessed in Raw264.7 macrophages. The effect on the transcription levels of *Hmox1*, a central player in detoxification of electrophilic and oxidative stresses, was also evaluated. The biological assays were carried out considering the effect of both acute (24 h) and chronic (3 weeks) exposures to aerosol WSOM, with the latter at maximal theoretical WSOM doses (*i.e.*, considering the average human air intake per hour, and the atmospheric water-soluble organic carbon concentrations in day-night cycles). Investigating the potential impact of aerosol WSOM composition on human health is essential, particularly when experiencing serious pollution conditions. This study set the basis for further understanding of the mechanisms of fine aerosol WSOM-induced respiratory diseases and may contribute to the development of targeted $PM_{2.5}$ regulations.

MATERIALS AND METHODS

Aerosol sampling and extraction of WSOM samples

The $PM_{2.5}$ samples were collected on a rooftop (*c.a.* 20 m above the ground) at the campus of University of Aveiro (40°38'N, 8°39'W), which is located about 10 km from the Atlantic coast on the outskirts of the city of Aveiro. The sampling site is impacted by both marine air masses travelling from the Atlantic Ocean and anthropogenic emissions from vehicular transport, residential, and industrial sources.[30,32,41] Episodes of increased $PM_{2.5}$ and WSOM concentrations are common in this area during colder periods and they can last several days,[29,30,41] allowing the collection of enough amount of aerosol WSOM within relatively short periods of time. The $PM_{2.5}$ samples were collected from 14 to 29 November 2016 (Autumn) and 27 March to 04 April 2016 (Spring), during the weekdays (*i.e.*, from Monday to Friday) in two distinct time periods: (i) daytime: 9:40 a.m. to 5:30 p.m. (Autumn)/6:30 p.m. (Spring), and (ii) overnight: 5:40 p.m. (Autumn)/6:40 p.m. (Spring) to 9:30 a.m. The $PM_{2.5}$ samples were collected on pre-fired quartz-fiber filters

(20.3×25.4 cm; Whatman QM-A) with an airflow rate of 1.13 m^3 min^{-1}. Additional details on aerosol sampling procedure are available in Section S1, in Supporting Information (SI). After sampling, the filter samples were folded in two, wrapped in aluminum foil and immediately transported to the laboratory, where they were weighted and stored frozen until further analysis. The meteorological data recorded during $PM_{2.5}$ collection is available in Table S1 (SI). The determination of organic carbon (OC) and elemental carbon (EC) in each $PM_{2.5}$ sample was performed by means of a Lab OC-EC Aerosol Analyzer (Sunset Laboratory Inc.) following a thermo-optical method, described in section S2 (SI).

An area of 315 cm^2 of each quartz filter was extracted with 150 mL of ultra-pure water (18.2 MΩ cm, filter area to water volume ratio of 2.1 cm^2 mL^{-1}) by mechanical stirring for 5 min followed by ultrasonic bath for 15 min. Each final aqueous slurry was filtered through a hydrophilic polyvinylidene fluoride membrane filter (Durapore®, Millipore, Ireland) of 0.22 μm pore size. At the end of this filtration step, the slurry residue was washed twice with 20 mL of ultrapure water in order to remove any water-soluble organic carbon (WSOC) still loosely bound to the filter residues. The dissolved organic carbon content of

each aqueous extract was measured by means of a Skalar (Breda, Netherlands) San++ Automated Wet Chemistry Analyzer, based on a UV-persulfate oxidation method.[42] After the WSOC extraction, and to obtain sufficient amount of WSOM samples for both NMR and biological assay studies, the aqueous aerosol extracts from each sampling period within each season were batched together, on a total of four pooled WSOM samples representative of day and nighttime conditions in Autumn and Spring seasons. Each pooled WSOM sample was further divided into two aliquots of similar volume: one aimed to NMR analysis and the other to biological assay studies. The aliquots were freeze-dried, and the obtained residues (designated as “whole aerosol WSOM sample”) were kept in a desiccator over silica gel until further analysis. Additional details on aerosol WSOM samples processing are available in Figure S1, section S3 (SI).

Liquid-state 1D and 2D NMR spectroscopy

All NMR spectra were acquired using a Bruker Avance-500 spectrometer operating at 500.13 and 125.77 MHz for ^{1}H and ^{13}C, respectively, and equipped with a liquid nitrogen cooling CryoProbe Prodigy™. All 1D and 2D spectra were run at 295.1 K, and additional

details on NMR data acquisition can be found in Section S4, in SI. The dried WSOM samples (7 to 3 mg) were dissolved in deuterated methanol (MeOH-d_4, ~1 mL) and transferred to 5 mm NMR tubes. The identification of functional groups in the NMR spectra was based on their chemical shift relative to solvent (MeOH-d_4) peak set at δ_H 3.31 ppm and δ_C 49.0 ppm. The interpretation of the spectral regions and structural assignments were based on the NMR chemical shift data described in the literature for standard organic compounds and for natural organic matter from different environmental matrices,[28,32,34,43,44] as well as on data generated by NMR simulators software's and databases (namely, Perkin Elmer ChemBioDraw® Ultra 14.0 and nmrdb.org).[45]

Cell culture and treatments

Raw 264.7, a mouse leukaemic monocyte macrophage cell line from American Type Culture Collection (ATCC number: TIB-71), was cultured in Dulbecco's Modified Eagle Media (DMEM) supplemented with 10% non-inactivated fetal bovine serum, 100 U mL^{-1} of penicillin, and 100 µg mL^{-1} streptomycin at 37°C in a humidified atmosphere of 95% air and 5% CO_2. For acute exposure experiments (4 to 24 h) cells were plated, let stabilize

overnight and then treated with indicated WSOC concentrations. In prolonged exposure experiments the cells were treated for 21 days, twice a day, with maximal theoretical inhaled doses of WSOC calculated from an mean inspired air volume of 8.64 m^3 per day: for Autumn season experiments, the cells were treated in the morning with 7.8 μg of daytime WSOC extract, and at the evening with 16.2 μg of nighttime extract; in Spring season experiments, the cells were treated in the morning with 5.6 μg of daytime WSOC extract and at the evening with 6.1 μg of nighttime extract. The cell treatments in the morning and evening were timed to mimic the schedule of $PM_{2.5}$ samples collection, whereas the cell medium was completely replaced every 2 days.

Nitric oxide (NO) production and *in vitro* antioxidant activity

The production of NO was measured by the accumulation of nitrite in the culture supernatants, using a colorimetric reaction with the Griess reagent as previously described.[46] In some of the experiments, it was assessed whether exposure to WSOM extracts affects the capacity of macrophages to respond to the strong pro-inflammatory stimuli bacterial LPS. In acute exposure experiments cells were pre incubated for 1 h with

178 WSOM extracts and then 1 μg mL^{-1} LPS was added following an incubation period of 24
179 h. In prolonged exposure experiments cells were treated for 21 days with WSOM extracts
180 and then stimulated for additional 24h with 1 μg mL^{-1} LPS. The effect of WSOM extracts
181 on the modulation of LPS-induced cellular oxidative stress was also addressed. Briefly,
182 Raw cells were plated at 0.05x10^6 per well in a μ-Chamber slide (IBIDI GmbH,
183 Germany), allowed to stabilize overnight and then stimulated with 1 μg mL^{-1} LPS during
184 24 h. The WSOM extracts were added 1 h prior to LPS stimulation. At the end of
185 incubation period, cells were washed three times and then loaded with 5 μM H_2DCFDA
186 and 0.5 μg mL^{-1} Hoechst in Hank's Balanced Salt Solution (HBSS) for 30 min at 37 ºC in
187 the dark. Cells were washed three times with HBSS and analyzed with an Axio Observer
188 Z1 fluorescent microscope (Zeiss Group, Oberkochen, Germany) at 63X magnification.
189

190 **Analysis of gene expression by q-PCR**

191 After cell treatment for the indicated times, total RNA was isolated with TRIzol reagent
192 according to the manufacturer's instructions. For analysis of mRNA levels of selected
193 genes, 1 μg of total RNA was reverse-transcribed using the iScript Select cDNA Synthesis

Kit and then real-time quantitative PCR (qPCR) reactions were performed using SYBR Green on a Bio-Rad CFX Connect device. The results were normalized using *Hprt1* as reference gene and presented as fold change relatively to untreated cells. Primer sequences were designed using Beacon Designer software version 8 (Premier Biosoft International, Palo Alto, CA, USA) and thoroughly tested.

Statistical analysis

Since aerosol WSOM samples were pooled and analyzed together, it should be mentioned that the cellular responses and PCR data were obtained for each pooled WSOM sample. However, at least three independent biological experiments were carried out for each sample. Results are presented as mean ± the standard deviation (SD) of the indicated number of experiments. Comparisons between two groups were made by the two-sided unpaired Student's *t* test and multiple group comparisons by One-Way ANOVA analysis, with a Dunnett's Multiple Comparison post-test. Statistical analysis was performed using GraphPad Prism, version 6 (GraphPad Software, San Diego, CA, USA). Significance levels are as follows: $*p<0.05$, $**p<0.01$, $***p<0.001$, $****p<0.0001$.

210

211

212 ## RESULTS AND DISCUSSION

213 ### Water-solubility of fine urban organic aerosols

214 The ambient concentrations of $PM_{2.5}$, OC, EC, and WSOC follow the same seasonal
215 trend, with the highest levels being found during Autumn (Table 1, and Figures S2 to S5
216 in SI). This seasonal trend has been quite well documented in this and other
217 regions,[28,30,33,37] although an opposite trend has been observed in North America.[47,48] In
218 Autumn, the median $PM_{2.5}$ concentration increased 1.5 fold during nighttime compared
219 with daytime, which is likely due to a lower mixing height and more stable atmospheric
220 conditions during the nighttime as well as increased emissions from residential heating
221 sources. These events could also explain the 3.3 and 3.6 fold increase in OC and WSOC
222 concentrations, respectively, during nighttime. In Spring, the diurnal variations of the
223 median OC and WSOC concentrations were evident, but the median concentration values
224 of these carbonaceous fractions only increased 1.3 and 1.5 fold, respectively, during
225 nighttime, whereas no major difference was observed for the $PM_{2.5}$ levels. Interestingly,

the OC-day/OC-night, EC-day/EC-night, and WSOM-day/WSOM-night ratios increased from a range of 0.34 – 0.71, 0.14 – 0.72, and 0.40 – 0.65, respectively, between the 27th and 29th of March, to 1.2 – 2.7, 0.8 – 1.8, and 1.1 – 2.1, respectively, between 30th of March and 6th of April (Figures S3 to S5, SI). This increase could be explained by a decrease in the OC, EC and WSOC concentrations during nighttime in the second half of the sampling period. During this period, the median values of temperature and maximum wind velocity raised from 13 to 15ºC and 2.7 to 4.0 m s^{-1}, respectively, leading to a more turbulent atmosphere and less emissions from anthropogenic activities related to house heating and, therefore, to a decrease in the nighttime OC, EC and WSOC concentrations. Furthermore, it is also likely that an additional OC source was present in daytime Spring samples, which cannot be explained solely by changes in primary emissions in view of the decrease of EC concentrations compared with Autumn. Considering that photo-oxidative capacity of atmosphere might be enhanced in Spring,[28,29] *in situ* production of secondary OC or chemical aging of insoluble primary organics could likely contribute to this additional OC. This enhanced photochemical activity can also explain the higher WSOC/OC ratios of Spring samples compared to those of Autumn samples.

<TABLE 1 here>

Day-night variability of aerosol WSOM features

Figure 1(A) shows the ^{1}H NMR spectra of pooled aerosol WSOM samples representative of day and nighttime conditions in Autumn and Spring seasons. These ^{1}H NMR spectra exhibit a remarkable similarity to those of other urban aerosol WSOM samples,[28,30–32] comprising a complex overlapping profile with broad bands superimposed by a relatively small number of sharp peaks. For a further understanding of these spectral profiles, a quantitative integration of the four main regions assigned to different types of non-exchangeable organic hydrogen [Figure 1(A)] was performed in order to assess the abundance of each functionality in WSOM samples. As depicted in Figure 1(B), and regardless of the sampling period, the saturated aliphatic protons (H–C) are typically the most important component, followed by unsaturated (H–C–C=) and oxygenated (H–C–O) aliphatic protons, and a less contribution from aromatic protons (Ar–H). Comparison between daytime and nighttime WSOM samples are expected to vary somewhat within both seasons, due to the distinctly different emission sources and atmospheric oxidation

conditions. However, in Spring, very little day-night variability was observed for the NMR structural signatures identified in the WSOM samples. On the other hand, in Autumn, the aliphatic H–C structures exhibit a distinct maximum (45%) for day aerosol WSOM and a minimum (34%) for the night sample. Additional differences between day and night WSOM samples in Autumn are found in the spectral regions associated with protons bound to oxygenated aliphatic (H–C–O) and aromatic (Ar–H) structures, whose contributions are higher for WSOM collected overnight (29% and 11%, respectively) than in WSOM collected in daytime (19% and 6.8%, respectively). The occurrence of strong H–C–O and aromatic signatures overnight in Autumn may be associated with the contribution of fresh biomass burning emissions for house heating under low air temperature conditions.[28,30,31] Moreover, the presence of an intense sharp resonance at δ ^{1}H 5.3 ppm [Figure 1(A)] attributed to protons bound to anomeric carbons [O–C(H)–O], such as those of anhydrosugars (e.g., levoglucosan and mannosan), which are known molecular markers of wood burning emissions,[30,32] further confirms the presence of smoke particles during this period.

<FIGURE 1 here>

The compositional day-night variability of aerosol WSOM samples within the two seasonal periods were further ascertain using 2D NMR spectroscopy (Figures S6 to S8, in SI). The ^{1}H-^{13}C HSQC NMR spectra of all WSOM samples reveal several important ^{1}H-^{13}C correlations in three major regions of chemical environments (Figures S6 and S7), but with very different relative intensities: aliphatic (δ_H 0.4–3.6 ppm/δ_C 10–45 ppm, represented by H–C and H–C–C=), *O*-alkyl (δ_H 3.6–6.0 ppm/δ_C 50–107 ppm, including anomeric carbons), and aromatic (δ_H 6.5–8.5 ppm/ δ_C 107–160 ppm) regions. The structural assignments of the 2D NMR cross peaks within these three chemical shift areas were further carried out based on spectral data from previous 2D NMR studies of aerosol WSOM samples.[30,32,34,49] The main structural findings are shown in the expanded aliphatic, *O*-alkyl, and aromatic regions of the ^{1}H-^{13}C HSQC NMR spectra in Figures S9 to S20 in SI. Overall, 15 polyfunctional aliphatic and aromatic substructures were identified in this study as being common to all aerosol WSOM samples, whereas 4 aromatic substructures were typical of aerosol WSOM sample collected overnight in Autumn (Figure S21, in SI). The presence of these 4 typical aromatic substructures [structures (18) to (21) in Figure S21] in overnight Autumn WSOM

290 sample confirm the notable influence of biomass burning emissions into the aerosol
291 WSOM characteristics during this period.[30,32] Five carbohydrate-like structures [structures
292 (11) to (15), in Figure S21] were consistently found in all aerosol WSOM samples, but
293 particularly more prominent in samples collected overnight in Autumn. Except for
294 trehalose [structure (13) in Figure S21], usually referred as a tracer for the resuspension
295 of surface soil and unpaved road dust,[50] the presence of the anhydrosugars levoglucosan
296 and mannosan [structures (11) and (12), respectively, Figure S21] and disaccharides
297 maltose and sucrose [structures (14) and (15), respectively, Figure S21] further confirm
298 that biomass burning is an important contributor to aerosol WSOM collected overnight in
299 Autumn.[30,32] The presence in all WSOM samples of NMR fingerprints assigned to DMA^+,
300 DEA^+ and MSA [structures (7) to (9) in Figure S21], and terephthalic acid [structure (16)
301 in Figure S21] also pinpoint to the contribution of, respectively, marine organic aerosols[30]
302 and oxidized aromatic hydrocarbons from urban traffic emissions[30,32] to aerosol WSOM
303 samples. Despite relatively uniform seasonal distribution of aliphatic structures among all
304 aerosol WSOM samples, there are actually important differences in the aromatic and *O*-
305 alkyl composition of nighttime aerosol WSOM samples in Autumn [summarized in Figure

306 1(C)]. These differences in WSOM chemical composition are expected to exert dissimilar
307 contribution on the oxidative and pro-inflammatory effects of air organic particles.

308 **Cytotoxicity of aerosol WSOM and impact on macrophages ROS and NO production**

309 Understanding the interaction between airway cellular populations and atmospheric air
310 particles, as well as the mechanisms through which their constituents cause inflammation
311 and cellular redox imbalances is of major importance. Therefore, the cytotoxicity of
312 aerosol WSOM over macrophages was firstly assessed in the WSOC concentration range
313 of 1 to 100 $\mu g\ mL^{-1}$, allowing to conclude that none caused a significant decrease in cell
314 viability (Section S7, Figure S22). Treatments with LPS or LPS + WSOM are also devoid
315 of significant impact on macrophages viability (Section S7, Figure S23). As NO is a key
316 molecule in inflammation and to the macrophage capacity to destroy invading pathogens,
317 the ability of WSOM to induce NO production and to modulate the LPS-induced
318 production in these cells was also analyzed. As shown in Figure S24(A), Section S8, day
319 and night WSOM Autumn samples at higher concentrations slightly induce NO
320 production. This is in agreement with previous reports showing small increases in NO
321 release by macrophages treated with particle or water-soluble fraction of $PM_{2.5}$.[51,52]

322 Furthermore, it can be perceived a different trend between the two WSOM samples: while
323 the day Autumn WSOM extract causes a concentration dependent increase in NO
324 production, the night extract has an opposite behavior. We hypothesize that the night
325 Autumn WSOM may contain organic compounds that induce NO, but also other
326 constituents that counteract this effect. Regarding the effects of Spring WSOM samples,
327 only day samples significantly induce NO release [Figure S24(A)]. Discrepancies between
328 the biological effects of $PM_{2.5}$ and its WSOM fraction collected during day or night are still
329 poorly documented, but the impact of seasonal variations in $PM_{2.5}$ chemical composition
330 (*e.g.* inorganic ions, elements and PAHs) and cytotoxicity has been extensively
331 covered.[53–55]
332 Interestingly, the effects of WSOM samples on the LPS-induced NO production was
333 significantly inhibited by all the samples at the concentration of 75 μg mL^{-1} [Figure
334 S24(B)]. This effect was not due to a direct NO scavenging activity (Figure S25), but
335 instead it may be the result of a modulation of inducible nitric oxide synthase (iNOS)
336 activity or gene transcription. Additionally, WSOM samples *per se* do not induced
337 oxidative stress, and surprisingly were able to markedly inhibit the LPS-triggered ROS

production in treated macrophages (Figure 2). These results differ from several reports where atmospheric particulate matter (PM) were shown to exert pro-oxidative effects.[17,56–58] These discrepancies may be explained by the differences in the material actually used since most of the available studies employ the whole air PM, or instead it could be due to considerable differences in the chemical composition of WSOM samples. The pro-oxidative characteristics of PM can be therefore mainly attributed to direct physical interactions with the particles themselves, or to their content in elements such as Cu, Cr, Pb, Co, Ni, or even WSOC.[17,58] It should be mentioned that the concentration of water-soluble elements and metals in the aqueous $PM_{2.5}$ extracts here studied are lower than those identified in the literature as exerting biological effects (Section S9, Table S2), thus supporting the assumption that the effects observed in this work are mainly due to an exposure to aerosol WSOM.

<FIGURE 2 here>

The inhibitory effect on the capacity of macrophages to produce ROS reported in this study is paradoxical: it may be beneficial given that it limits an inflammatory reaction;

353 however, it can compromise the efficacy of macrophages to destroy harmful
354 microorganisms during an infection by limiting the oxidative burst.
355
356
357 **Effects of aerosol WSOM on the modulation of macrophage inflammatory status**
358 Based on the results obtained thus far, the potential anti-inflammatory activity of aerosol
359 WSOM samples was also explored. For this, the impact of WSOM samples on the
360 transcription of *Il1b*, *Nos2* (pro-inflammatory genes) and *Hmox1* (anti-
361 inflammatory/cytoprotective), or in the modulation of their LPS-induced transcription was
362 evaluated. As shown in Figure S26, Section S10, Autumn and Spring WSOM samples
363 present a similar profile, although with different magnitudes. *Hmox1* transcription is
364 induced either by day or night samples in a dose dependent way. This observation agrees
365 with previous reports where PAHs present in PM (fine and coarse) were shown to induce
366 *Hmox1* transcription.[2,59,60] *Hmox* is a detoxifying enzyme that is expressed in response to
367 oxidative and electrophilic stresses as the result of the activation of the Keap/Nrf2
368 signaling pathway.[61] Therefore, the observed increases indicate that WSOM samples contain

electrophilic compounds, of which substructures (1) and (8) to (10) in Figure 1(C) might be suitable candidates.

Regarding the modulation of *Il1b* and *Nos2* transcription, once again Autumn and Spring WSOM samples presented a similar profile, with moderate increases being induced (Figure S26). These results are in agreement with previous studies where the exposure to $PM_{2.5}$ was shown to increase the transcription of *Il1b* and *Nos2* genes in the same cell model, causing a moderate pro-inflammatory effect.[60,62] In this study, when comparing day and night WSOM samples, there are clear differences: while for day WSOM, the increase in samples concentration is followed by an increase in the transcription of referred genes, the opposite occurs for night samples (Figure S26). This explains the lower production of NO in cells treated with higher concentrations of night WSOM samples [Figure S24(A)]. Regarding the cells treated with LPS, although all the tested WSOM samples have slight pro-inflammatory properties, they downregulate the LPS-induced inflammatory state by increasing *Hmox1* and reducing *Il1b* and *Nos2* transcription (Figure 3). Similar profiles were found when the levels of these proteins were analyzed by western blot (Section S11, Figure S27). The increase in *Hmox1* transcription and respective protein expression in addition to the intrinsic antioxidant characteristics of the WSOM samples support their strong capacity to prevent LPS-induced oxidative stress. In turn, the decrease in the LPS-induced *Nos2*

transcription (Figures 3) resulted in a downregulation of the iNOS protein levels (Figure S27), which can explain the observed decrease of LPS-induced NO production in cells pre-treated with WSOM extracts. This capacity to limit LPS-induced inflammatory status was not due to impairment of NF-κB nuclear translocation (Section S12, Figure S28). Given that MAPKs signaling pathways were also shown to modulate PM-induced inflammation,[63,64] the effects of WSOM extracts on the phosphorylation levels of p38, JNK and ERK (Section S13, Figure S29) were also assessed. While ERK was not affected and JNK marginally activated, LPS-induced activation of p38MAPK signaling cascade was downmodulated by exposure to extracts, particularly to nighttime WSOM samples (Figure S29). This impairment of p38 MAPK activation may be in part responsible for the observed decrease in LPS-triggered inflammatory status. Additionally, contributing to this impaired capacity of macrophages to mount an adequate inflammatory response, the extracts may be causing alterations in the cellular cytoskeleton, impairing the traffic of secretory vesicles and the release of cytokines, in a process similar to the one recently described by Longhin and collaborators.[65]

<FIGURE 3 here>

Given that all experiments were performed with relatively high WSOC concentrations within an acute exposure setup, it was decided to analyze the effects of chronic exposure by culturing cells during 3 weeks with maximal theoretical aerosol WSOM doses. For this, the average human air intake per hour and the atmospheric WSOC concentrations during day and nighttime conditions were taken into account for administrating maximal

theoretical WSOC quantities in day-night cycles. As demonstrated in Figure 4(A), cells exposed to aerosol WSOM exhibit a slight increase in the transcription of *Hmox1*, *Il1b*, and *Nos2* genes. When these cells chronically exposed to WSOM samples were then treated with LPS, the *Hmox1* and *Nos2* slightly increased, but the mRNA levels of *Il1b* were significantly down modulated [Figure 4(B)]. While this small increase observed in *Nos2* transcription does not reach statistical significance it reveals an opposite tendency to the one observed in acute experiments. We hypothesize that this may be mainly due the highly different applied WSOC concentrations and to the presence in the extracts of pro and anti-inflammatory compounds. In acute experiments the concentration of compounds with anti-inflammatory properties may reach a level enough to impair LPS-triggered signaling pathways, namely those regulating *Nos2* transcription. In contrast, in prolonged exposure experiments, the cells were continuously treated with very low amounts of WSOM extracts and the compounds with pro-inflammatory properties may prime cells rendering them more responsive to posterior LPS stimulation. Therefore, prolonged exposure to even very small concentrations of water-soluble organic

422 compounds present in $PM_{2.5}$, can cause a decrease in the capacity of macrophages to
423 respond to a subsequent inflammatory stimulus.

424 <FIGURE 4 here>

425 In summary, the set of data provided by 1D and 2D NMR analysis indicates that the fine
426 aerosol WSOM samples hold similar functional groups; however, they differ in terms of
427 their relative distribution both between seasons and in a day-night cycle. This study also
428 highlights that the compositional features of aerosol WSOM samples correlates with their
429 ability to induce a moderate inflammatory status in macrophages, which at long-term may
430 compromise their capacity to mount an effective inflammatory response required to
431 manage harmful pathogens. Therefore, continuous and prolonged exposure to aerosol
432 water-soluble organic compounds could result in increased susceptibility to respiratory
433 infections. For a better understanding of the overall ability of fine aerosol WSOM to exert
434 pro-inflammatory effects, further studies should be conducted involving a larger data set
435 of different WSOM samples, while effectively segregating the contributions from different
436 WSOM constituents.

437

438

439 ASSOCIATED CONTENT

440 **Supporting Information**. Experimental procedure for $PM_{2.5}$ sampling, meteorological
441 information collected during each sampling campaign, experimental details for OC and
442 EC analysis, average ambient concentrations of the main aerosol carbon fractions, 2D
443 NMR data acquisition and 2D NMR spectral assignments of the aerosol WSOM samples,
444 water-soluble elements and metals concentrations in $PM_{2.5}$ samples, impact of aerosol
445 WSOM samples on macrophages viability, NO production and scavenging activity,
446 modulation of macrophage inflammatory status, protein levels of iNOS, HMOX1, and IL-
447 1β, activation of pro-inflammatory NF-κB signaling pathways, and modulation of MAPKs
448 signaling pathways. This material is available free of charge via the Internet at
449 http://pubs.acs.org.

450

451

452

453 AUTHOR INFORMATION

454 Corresponding Author

455 *E-mail: regina.duarte@ua.pt: Phone: +351 234 370 360.

456 **Author Contributions**

457 The manuscript was written through contributions of all authors and all authors have given

458 approval to its final version. § Bruno M. Neves and Regina M.B.O. Duarte supervised this study

459 equally as senior authors.

460 ORCID: Antoine S. Almeida: 0000-0002-4535-1213; Rita M.P. Ferreira: 0000-0002-6872-

461 4051; Artur M.S. Silva: 0000-0003-2861-8286; Armando C. Duarte: 0000-0002-4868-

462 4099; Bruno M. Neves: 0000-0001-7391-3124; Regina M.B.O. Duarte: 0000-0002-1825-

463 6528.

464

465 **Notes**

466 The authors declare no competing financial interest.

467

468 ACKNOWLEDGMENT

Thanks are due to FCT/MCTES for the financial support to CESAM (UID/AMB/50017/2019), Organic Chemistry Research Unit (QOPNA, UID/QUI/00062/2019), and iBiMED (UID/BIM/04501/2013 and UID/BIM/04501/2019), and Portuguese NMR network, through national funds. FCT/MCTES is also acknowledged for an Investigator FCT Contract (IF/00798/2015). The Authors would like to acknowledge Catarina Leitão for her assistance on the western blot experiments.

REFERENCES

(1) Mills, N. L.; Donaldson, K.; Hadoke, P. W.; Boon, N. A.; MacNee, W.; Cassee, F. R.; Sandström, T.; Blomberg, A.; Newby, D. E. Adverse Cardiovascular Effects of Air Pollution. *Nat. Clin. Pract. Cardiovasc. Med.* **2009**, *6* (1), 36–44.

(2) Feng, S.; Gao, D.; Liao, F.; Zhou, F.; Wang, X. The Health Effects of Ambient PM2.5 and Potential Mechanisms. *Ecotoxicol. Environ. Saf.* **2016**, *128*, 67–74.

(3) Li, R.; Zhou, R.; Zhang, J. Function of PM2.5 in the Pathogenesis of Lung Cancer and Chronic Airway Inflammatory Diseases. *Oncol. Lett.* **2018**, *15* (5), 7506–7514.

485 (4) Santibáñez-Andrade, M.; Quezada-Maldonado, E. M.; Osornio-Vargas, Á.;
486 Sánchez-Pérez, Y.; García-Cuellar, C. M. Air Pollution and Genomic Instability: The
487 Role of Particulate Matter in Lung Carcinogenesis. *Environ. Pollut.* **2017**, *229*, 412–
488 422.
489 (5) Basagaña, X.; Esnaola, M.; Rivas, I.; Amato, F.; Alvarez-Pedrerol, M.; Forns, J.;
490 López-Vicente, M.; Pujol, J.; Nieuwenhuijsen, M.; Querol, X.; Sunyer, J.
491 Neurodevelopmental Deceleration by Urban Fine Particles from Different Emission
492 Sources : A Longitudinal Observational Study. *Environ. Health Perspect.* **2016**, *124*
493 (10), 1630–1636.
494 (6) Calderón-Garcidueñas, L.; Kulesza, R. J.; Doty, R. L.; Angiulli, A. D.; Torres-
495 Jardón, R. Megacities Air Pollution Problems : Mexico City Metropolitan Area
496 Critical Issues on the Central Nervous System Pediatric Impact. *Environ. Res.*
497 **2015**, *137*, 157–169.
498 (7) Suades-González, E.; Gascon, M.; Guxens, M.; Sunyer, J. Air Pollution and
499 Neuropsychological Development: A Review of the Latest Evidence. *Endocrinology*
500 **2015**, *156* (10), 3473–3482.

(8) Gosset, P.; Aboukais, A.; Dagher, Z.; Shirali, P.; Ledoux, F.; Surpateanu, G.; Garçon, G.; Courcot, D.; Puskaric, E. Pro-Inflammatory Effects of Dunkerque City Air Pollution Particulate Matter 2.5 in Human Epithelial Lung Cells (L132) in Culture. *J. Appl. Toxicol.* **2005**, *25* (2), 166–175.

(9) Sun, Q.; Chen, L. C.; Briazova, T.; Laing, S.; Zhang, K.; Wang, G.; Wang, A.; Gow, A.; Zhang, C.; Chen, A. F.; Rajagopalan, S.; Chen, L. C.; Sun, Q.; Zhang, K. Airborne Particulate Matter Selectively Activates Endoplasmic Reticulum Stress Response in the Lung and Liver Tissues. *Am. J. Physiol. Physiol.* **2010**, *299* (4), C736–C749.

(10) Liu, Q.; Baumgartner, J.; Zhang, Y.; Liu, Y.; Sun, Y.; Zhang, M. Oxidative Potential and Inflammatory Impacts of Source Apportioned Ambient Air Pollution in Beijing. *Environ. Sci. Technol.* **2014**, *48* (21), 12920–12929.

(11) Pope, C. A.; Dockery, D. W. Health Effects of Fine Particulate Air Pollution: Lines That Connect. *J. Air Waste Manag. Assoc.* **2006**, *56* (6), 709–742.

(12) Visentin, M.; Pagnoni, A.; Sarti, E.; Pietrogrande, M. C. Urban PM2.5 Oxidative Potential: Importance of Chemical Species and Comparison of Two

517 Spectrophotometric Cell-Free Assays. *Environ. Pollut.* **2016**, *219*, 72–79.

518 (13) Huang, Q.; Zhang, J.; Peng, S.; Tian, M.; Chen, J.; Shen, H. Effects of Water
519 Soluble PM2.5 Extracts Exposure on Human Lung Epithelial Cells (A549): A
520 Proteomic Study. *J. Appl. Toxicol.* **2014**, *34* (6), 675–687.

521 (14) Fang, T.; Verma, V.; T Bates, J.; Abrams, J.; Klein, M.; Strickland, J. M.; Sarnat, E.
522 S.; Chang, H. H.; Mulholland, A. J.; Tolbert, E. P.; Russel, G. A.; Weber, J. R.
523 Oxidative Potential of Ambient Water-Soluble PM2.5 in the Southeastern United
524 States: Contrasts in Sources and Health Associations between Ascorbic Acid (AA)
525 and Dithiothreitol (DTT) Assays. *Atmos. Chem. Phys.* **2016**, *16* (6), 3865–3879.

526 (15) Cassee, F. R.; Héroux, M.-E.; Gerlofs-Nijland, M. E.; Kelly, F. J. Particulate Matter
527 beyond Mass: Recent Health Evidence on the Role of Fractions, Chemical
528 Constituents and Sources of Emission. *Inhal. Toxicol.* **2013**, *25* (14), 802–812.

529 (16) MohseniBandpi, A.; Eslami, A.; Shahsavani, A.; Khodagholi, F.; Alinejad, A.
530 Physicochemical Characterization of Ambient PM2.5 in Tehran Air and Its Potential
531 Cytotoxicity in Human Lung Epithelial Cells (A549). *Sci. Total Environ.* **2017**, *593*,
532 182–190.

533 (17) Saffari, A.; Daher, N.; Shafer, M. M.; Schauer, J. J.; Sioutas, C. Global Perspective
534 on the Oxidative Potential of Airborne Particulate Matter: A Synthesis of Research
535 Findings. *Environ. Sci. Technol.* **2014**, *48* (13), 7576–7583.
536 (18) Janssen, N. A. H.; Yang, A.; Strak, M.; Steenhof, M.; Hellack, B.; Gerlofs-Nijland,
537 M. E.; Kuhlbusch, T.; Kelly, F.; Harrison, R.; Brunekreef, B.; Hoek, G.; Cassee, F.
538 Oxidative Potential of Particulate Matter Collected at Sites with Different Source
539 Characteristics. *Sci. Total Environ.* **2014**, *472*, 572–581.
540 (19) Risom, L.; Møller, P.; Loft, S. Oxidative Stress-Induced DNA Damage by Particulate
541 Air Pollution. *Mutat. Res. Mol. Mech. Mutagen.* **2005**, *592* (1–2), 119–137.
542 (20) Saffari, A.; Daher, N.; Samara, C.; Voutsa, D.; Kouras, A.; Manoli, E.;
543 Karagkiozidou, O.; Vlachokostas, C.; Moussiopoulos, N.; Shafer, M. M.; Schauer,
544 J. J.; Sioutas, C. Increased Biomass Burning Due to the Economic Crisis in Greece
545 and Its Adverse Impact on Wintertime Air Quality in Thessaloniki. *Environ. Sci.*
546 *Technol.* **2013**, *47* (23), 13313–13320.
547 (21) Lin, P.; Yu, J. Z. Generation of Reactive Oxygen Species Mediated by Humic-like
548 Substances in Atmospheric Aerosols. *Environ. Sci. Technol.* **2011**, *45* (24), 10362–

549 10368.

550 (22) Verma, V.; Rico-Martinez, R.; Kotra, N.; King, L.; Liu, J.; Snell, T. W.; Weber, R. J.

551 Contribution of Water-Soluble and Insoluble Components and Their

552 Hydrophobic/Hydrophilic Subfractions to the Reactive Oxygen Species-Generating

553 Potential of Fine Ambient Aerosols. *Environ. Sci. Technol.* **2012**, *46* (20), 11384–

554 11392.

555 (23) Samara, C. On the Redox Activity of Urban Aerosol Particles: Implications for Size

556 Distribution and Relationships with Organic Aerosol Components. *Atmosphere*

557 *(Basel).* **2017**, *8* (10).

558 (24) Saffari, A.; Daher, N.; Shafer, M. M.; Schauer, J. J.; Sioutas, C. Seasonal and

559 Spatial Variation in Reactive Oxygen Species Activity of Quasi-Ultrafine Particles

560 (PM0.25) in the Los Angeles Metropolitan Area and Its Association with Chemical

561 Composition. *Atmos. Environ.* **2013**, *79*, 566–575.

562 (25) Verma, V.; Fang, T.; Xu, L.; Peltier, R. E.; Russell, A. G.; Ng, N. L.; Weber, R. J.

563 Organic Aerosols Associated with the Generation of Reactive Oxygen Species

564 (ROS) by Water-Soluble PM2.5. *Environ. Sci. Technol.* **2015**, *49* (7), 4646–4656.

565 (26) Dou, J.; Lin, P.; Kuang, B. Y.; Yu, J. Z. Reactive Oxygen Species Production
566 Mediated by Humic-like Substances in Atmospheric Aerosols: Enhancement
567 Effects by Pyridine, Imidazole, and Their Derivatives. *Environ. Sci. Technol.* **2015**,
568 *49* (11), 6457–6465.
569 (27) Zhang, Q.; Jimenez, J. L.; Canagaratna, M. R.; Allan, J. D.; Coe, H.; Ulbrich, I.;
570 Alfarra, M. R.; Takami, A.; Middlebrook, A. M.; Sun, Y. L.; Dzepina, K.; Dunlea, E.;
571 Docherty, K.; DeCarlo, P. F.; Salcedo, D.; Onasch, T.; Jayne, J. T.; Miyoshi, T.;
572 Shimono, A.; Hatakeyama, S.; Takegawa, N.; Kondo, Y.; Schneider, J.; Drewnick,
573 F.; Borrmann, S.; Weimer, S.; Demerjian, K.; Williams, P.; Bower, K.; Bahreini, R.;
574 Cottrell, L.; Griffin, R. J., Rautiainen, J.; Sun, J. Y.; Zhang, Y. M.; Worsnop, D. R.
575 Ubiquity and Dominance of Oxygenated Species in Organic Aerosols in
576 Anthropogenically-Influenced Northern Hemisphere Midlatitudes. *Geophys. Res.*
577 *Lett.* **2007**, *34* (13).
578 (28) Lopes, S. P.; Matos, J. T. V.; Silva, A. M. S.; Duarte, A. C.; Duarte, R. M. B. O. 1 H
579 NMR Studies of Water- and Alkaline-Soluble Organic Matter from Fine Urban
580 Atmospheric Aerosols. *Atmos. Environ.* **2015**, *119*, 374–380.

581 (29) Duarte, R. M. B. O.; Freire, S. M. S. C.; Duarte, A. C. Investigating the Water-
582 Soluble Organic Functionality of Urban Aerosols Using Two-Dimensional
583 Correlation of Solid-State 13C NMR and FTIR Spectral Data. *Atmos. Environ.* **2015**,
584 *116*, 245–252.
585 (30) Duarte, R. M. B. O.; Piñeiro-Iglesias, M.; López-Mahía, P.; Muniategui-Lorenzo, S.;
586 Moreda-Piñeiro, J.; Silva, A. M. S.; Duarte, A. C. Comparative Study of Atmospheric
587 Water-Soluble Organic Aerosols Composition in Contrasting Suburban
588 Environments in the Iberian Peninsula Coast. *Sci. Total Environ.* **2019**, *648*, 430–
589 441.
590 (31) Duarte, R. M. B. O.; Matos, J. T. V.; Paula, A. S.; Lopes, S. P.; Pereira, G.;
591 Vasconcellos, P.; Gioda, A.; Carreira, R.; Silva, A. M. S.; Duarte, A. C.; Smichowski,
592 P.; Rojas, N.; Sanchez-Ccoyllo, O. Structural Signatures of Water-Soluble Organic
593 Aerosols in Contrasting Environments in South America and Western Europe.
594 *Environ. Pollut.* **2017**, *227*, 513–525.
595 (32) Matos, J. T. V.; Duarte, R. M. B. O.; Lopes, S. P.; Silva, A. M. S.; Duarte, A. C.
596 Persistence of Urban Organic Aerosols Composition: Decoding Their Structural

597 Complexity and Seasonal Variability. *Environ. Pollut.* **2017**, *231*, 281–290.

598 (33) Duarte, R. M. B. O.; Santos, E. B. H.; Pio, C. A.; Duarte, A. C. Comparison of

599 Structural Features of Water-Soluble Organic Matter from Atmospheric Aerosols

600 with Those of Aquatic Humic Substances. *Atmos. Environ.* **2007**, *41*, 8100–8113.

601 (34) Duarte, R. M. B. O.; Silva, A. M. S.; Duarte, A. C. Two-Dimensional NMR Studies

602 of Water-Soluble Organic Matter in Atmospheric Aerosols. *Environ. Sci. Technol.*

603 **2008**, *42* (22), 8224–8230.

604 (35) Ng, N. L.; Canagaratna, M. R.; Zhang, Q.; Jimenez, J. L.; Tian, J.; Ulbrich, I. M.;

605 Kroll, J. H.; Docherty, K. S.; Chhabra, P. S.; Bahreini, R.; Murphy, S. M.; Seinfeld,

606 J. H.; Hildebrandt, L.; Donahue, N. M.; DeCarlo, P. F.; Lanz, V. A.; Prévôt, A. S. H.;

607 Dinar, E.; Rudich, Y.; Worsnop, D. R. Organic Aerosol Components Observed in

608 Northern Hemispheric Datasets from Aerosol Mass Spectrometry. *Atmos. Chem.*

609 *Phys.* **2010**, *10* (10), 4625–4641.

610 (36) Cleveland, M. J.; Ziemba, L. D.; Griffin, R. J.; Dibb, J. E.; Anderson, C. H.; Lefer,

611 B.; Rappenglück, B. Characterization of Urban Aerosol Using Aerosol Mass

612 Spectrometry and Proton Nuclear Magnetic Resonance Spectroscopy. *Atmos.*

Environ. **2012**, *54*, 511–518.

(37) Shakya, K. M.; Place, P. F.; Griffin, R. J.; Talbot, R. W. Carbonaceous Content and Water-Soluble Organic Functionality of Atmospheric Aerosols at a Semi-Rural New England Location. *J. Geophys. Res. Atmos.* **2012**, *117* (3), 1–13.

(38) Timonen, H.; Carbone, S.; Aurela, M.; Saarnio, K.; Saarikoski, S.; Ng, N. L.; Canagaratna, M. R.; Kulmala, M.; Kerminen, V.-M.; Worsnop, D. R.; Hillamo, R. Characteristics, Sources and Water-Solubility of Ambient Submicron Organic Aerosol in Springtime in Helsinki, Finland. *J. Aerosol Sci.* **2013**, *56*, 61–77.

(39) Chalbot, M.-C. G.; Brown, J.; Chitranshi, P.; Gamboa da Costa, G.; Pollock, E. D.; Kavouras, I. G. Functional Characterization of the Water-Soluble Organic Carbon of Size-Fractionated Aerosol in the Southern Mississippi Valley. *Atmos. Chem. Phys.* **2014**, *14* (12), 6075–6088.

(40) Paglione, M.; Saarikoski, S.; Carbone, S.; Hillamo, R.; Facchini, M. C.; Finessi, E.; Giulianelli, L.; Carbone, C.; Fuzzi, S.; Moretti, F.; Tagliavini, E.; Swietlicki, E.; Stenstrom, K. E.; Prévôt, A. S. H.; Massoli, P.; Canaragatna, M.; Worsnop, D.; Decesari, S. Primary and Secondary Biomass Burning Aerosols Determined by

629 Proton Nuclear Magnetic Resonance (1H-NMR) Spectroscopy during the 2008
630 EUCAARI Campaign in the Po Valley (Italy). *Atmos. Chem. Phys.* **2014**, *14* (10),
631 5089–5110.
632 (41) Duarte, R. M. B. O.; Matos, J. T. V.; Paula, A. S.; Lopes, S. P.; Ribeiro, S.; Santos,
633 J. F.; Patinha, C.; da Silva, E. F.; Soares, R.; Duarte, A. C. Tracing of Aerosol
634 Sources in an Urban Environment Using Chemical, Sr Isotope, and Mineralogical
635 Characterization. *Environ. Sci. Pollut. Res.* **2017**, *24* (12), 11006–11016.
636 (42) Lopes, C.; Abreu, S.; Válega, M.; Duarte, R.; Pereira, M.; Duarte, A. The
637 Assembling and Application of an Automated Segmented Flow Analyzer for the
638 Determination of Dissolved Organic Carbon Based on UV-Persulphate Oxidation.
639 *Anal. Lett.* **2006**, *39* (9), 1979-1992.
640 (43) Hertkorn, N.; Kettrup, A. Molecular Level Structural Analysis of Natural Organic
641 Matter and of Humic Substances by Multinuclear and Higher Dimensional NMR
642 Spectroscopy. In *Use of Humic Substances to Remediate Polluted Environments:*
643 *From Theory to Practice*; Perminova, I. V., Hatfield, K., Hertkorn, N., Eds.; Springer,
644 2005; pp 391–435.

(44) Simpson, A. J.; Burdon, J.; Graham, C. L.; Hayes, M. H. B.; Spencer, N.; Kingery, W. L. Interpretation of Heteronuclear and Multidimensional NMR Spectroscopy of Humic Substances. *Eur. J. Soil Sci.* **2001**, *52* (3), 495–509.

(45) Banfi, D.; Patiny, L. Www.Nmrdb.Org: Resurrecting and Processing NMR Spectra On-Line. *Chim. Int. J. Chem.* **2008**, *62* (4), 280–281.

(46) Morais, E. S.; Silva, N. H. C. S.; Sintra, T. E.; Santos, S. A. O.; Neves, B. M.; Almeida, I. F.; Costa, P. C.; Correia-Sá, I.; Ventura, S. P. M.; Silvestre, A. J. D.; Freire, M. G.; Freire, C. S. R Anti-Inflammatory and Antioxidant Nanostructured Cellulose Membranes Loaded with Phenolic-Based Ionic Liquids for Cutaneous Application. *Carbohydr. Polym.* **2019**, *206*, 187–197.

(47) Park, R. J.; Jacob, D. J.; Chin, M.; Martin, R. V. Sources of Carbonaceous Aerosols over the United States and Implications for Natural Visibility. *J. Geophys. Res.* **2003**, *108* (D12), 4355.

(48) Wozniak, A. S.; Bauer, J. E.; Dickhut, R. M. Characteristics of Water-Soluble Organic Carbon Associated with Aerosol Particles in the Eastern United States. *Atmos. Environ.* **2012**, *46*, 181–188.

661 (49) Schmitt-Kopplin, P.; Gelencsér, A.; Dabek-Zlotorzynska, E.; Kiss, G.; Hertkorn, N.;
662 Harir, M.; Hong, Y.; Gebefügi, I. Analysis of the Unresolved Organic Fraction in
663 Atmospheric Aerosols with Ultrahigh-Resolution Mass Spectrometry and Nuclear
664 Magnetic Resonance Spectroscopy: Organosulfates As Photochemical Smog
665 Constituents †. *Anal. Chem.* **2010**, *82* (19), 8017–8026.
666 (50) Simoneit, B. R. T.; Elias, V. O.; Kobayashi, M.; Kawamura, K.; Rushdi, A. I.;
667 Medeiros, P. M.; Rogge, W. F.; Didyk, B. M. Sugars - Dominant Water-Soluble
668 Organic Compounds in Soils and Characterization as Tracers in Atmospheric
669 Participate Matter. *Environ. Sci. Technol.* **2004**, *38* (22), 5939–5949.
670 (51) Jalava, P. I.; Salonen, R. O.; Pennanen, A. S.; Happo, M. S.; Penttinen, P.; Hälinen,
671 A. I.; Sillanpää, M.; Hillamo, R.; Hirvonen, M.-R. Effects of Solubility of Urban Air
672 Fine and Coarse Particles on Cytotoxic and Inflammatory Responses in RAW 264.7
673 Macrophage Cell Line. *Toxicol. Appl. Pharmacol.* **2008**, *229* (2), 146–160.
674 (52) Chauhan, V.; Breznan, D.; Goegan, P.; Nadeau, D.; Karthikeyan, S.; Brook, J. R.;
675 Vincent, R. Effects of Ambient Air Particles on Nitric Oxide Production in
676 Macrophage Cell Lines. *Cell Biol. Toxicol.* **2004**, *20* (4), 221–239.

677 (53) Becker, S.; Dailey, L. A.; Soukup, J. M.; Grambow, S. C.; Devlin, R. B.; Huang,
678 Y.-C. T. Seasonal Variations in Air Pollution Particle-Induced Inflammatory
679 Mediator Release and Oxidative Stress. *Environ. Health Perspect.* **2005**, *113* (8),
680 1032–1038.
681 (54) Longhin, E.; Pezzolato, E.; Mantecca, P.; Holme, J. A.; Franzetti, A.; Camatini, M.;
682 Gualtieri, M. Season Linked Responses to Fine and Quasi-Ultrafine Milan PM in
683 Cultured Cells. *Toxicol. In Vitro* **2013**, *27* (2), 551–559.
684 (55) Perrone, M. G.; Gualtieri, M.; Ferrero, L.; Lo Porto, C.; Udisti, R.; Bolzacchini, E.;
685 Camatini, M. Seasonal Variations in Chemical Composition and in Vitro Biological
686 Effects of Fine PM from Milan. *Chemosphere* **2010**, *78* (11), 1368–1377.
687 (56) Jalava, P. I.; Aakko-Saksa, P.; Murtonen, T.; Happo, M. S.; Markkanen, A.; Yli-
688 Pirilä, P.; Hakulinen, P.; Hillamo, R.; Mäki-Paakkanen, J.; Salonen, R. O.;
689 Jokiniemi, J.; Hirvonen, M.-R. Toxicological Properties of Emission Particles from
690 Heavy Duty Engines Powered by Conventional and Bio-Based Diesel Fuels and
691 Compressed Natural Gas. *Part. Fibre Toxicol.* **2012**, *9* (1), 37.
692 (57) Uski, O.; Jalava, P. I.; Happo, M. S.; Torvela, T.; Leskinen, J.; Mäki-Paakkanen, J.;

693 Tissari, J.; Sippula, O.; Lamberg, H.; Jokiniemi, J.; Hirvonen, M. R. Effect of Fuel
694 Zinc Content on Toxicological Responses of Particulate Matter from Pellet
695 Combustion in Vitro. *Sci. Total Environ.* **2015**, *511*, 331–340.
696 (58) Daher, N.; Ruprecht, A.; Invernizzi, G.; De Marco, C.; Miller-Schulze, J.; Heo, J. B.;
697 Shafer, M. M.; Shelton, B. R.; Schauer, J. J.; Sioutas, C. Characterization, Sources
698 and Redox Activity of Fine and Coarse Particulate Matter in Milan, Italy. *Atmos.*
699 *Environ.* **2012**, *49*, 130–141.
700 (59) Bachoual, R.; Boczkowski, J.; Goven, D.; Amara, N.; Tabet, L.; On, D.; Leçon-
701 Malas, V.; Aubier, M.; Lanone, S. Biological Effects of Particles from the Paris
702 Subway System. *Chem. Res. Toxicol.* **2007**, *20* (10), 1426–1433.
703 (60) Bekki, K.; Ito, T.; Yoshida, Y.; He, C.; Arashidani, K.; He, M.; Sun, G.; Zeng, Y.;
704 Sone, H.; Kunugita, N.; Ichinose, T. PM 2.5 Collected in China Causes
705 Inflammatory and Oxidative Stress Responses in Macrophages through the
706 Multiple Pathways. *Environ. Toxicol. Pharmacol.* **2016**, *45*, 362–369.
707 (61) Kobayashi, A.; Kang, M.-I.; Watai, Y.; Tong, K. I.; Shibata, T.; Uchida, K.;
708 Yamamoto, M. Oxidative and Electrophilic Stresses Activate Nrf2 through Inhibition

709 of Ubiquitination Activity of Keap1. *Mol. Cell. Biol.* **2006**, *26* (1), 221–229.

710 (62) Jalava, P. I.; Happo, M. S.; Huttunen, K.; Sillanpää, M.; Hillamo, R.; Salonen, R.

711 O.; Hirvonen, M.-R. Chemical and Microbial Components of Urban Air PM Cause

712 Seasonal Variation of Toxicological Activity. *Environ. Toxicol. Pharmacol.* **2015**, *40*

713 (2), 375–387.

714 (63) Wang, J.; Huang, J.; Wang, L.; Chen, C.; Yang, D.; Jin, M.; Bai, C.; Song, Y. Urban

715 Particulate Matter Triggers Lung Inflammation via the ROS-MAPK-NF-KB Signaling

716 Pathway. *J. Thorac. Dis.* **2017**, *9* (11), 4398–4412.

717 (64) Xiao, X.; Wang, R.; Cao, L.; Shen, Z.; Cao, Y. The Role of MAPK Pathways in

718 Airborne Fine Particulate Matter-Induced Upregulation of Endothelin Receptors in

719 Rat Basilar Arteries. *Toxicol. Sci.* **2016**, *149* (1), 213–226.

720 (65) Longhin, E.; Holme, J. A.; Gualtieri, M.; Camatini, M.; Øvrevik, J. Milan Winter Fine

721 Particulate Matter (WPM2.5) Induces IL-6 and IL-8 Synthesis in Human Bronchial

722 BEAS-2B Cells, but Specifically Impairs IL-8 Release. *Toxicol. Vitr.* **2018**, *52* (July),

723 365–373.

724

725

726 **TOC Art**

727

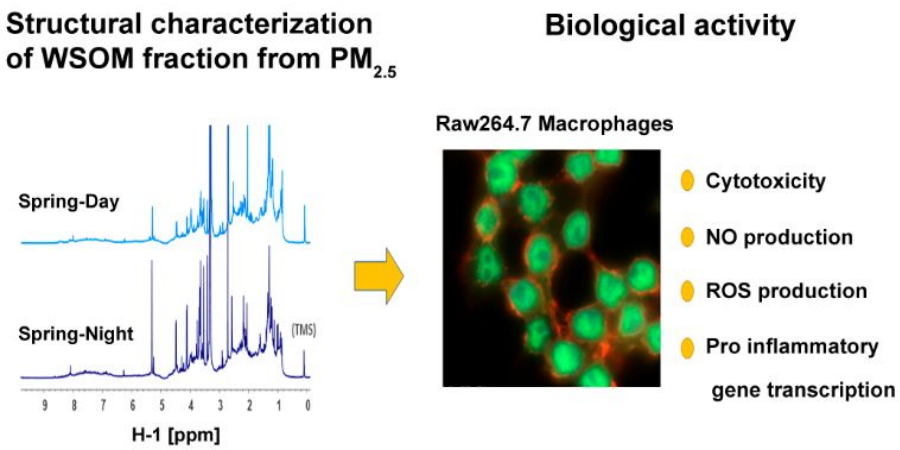

728

729

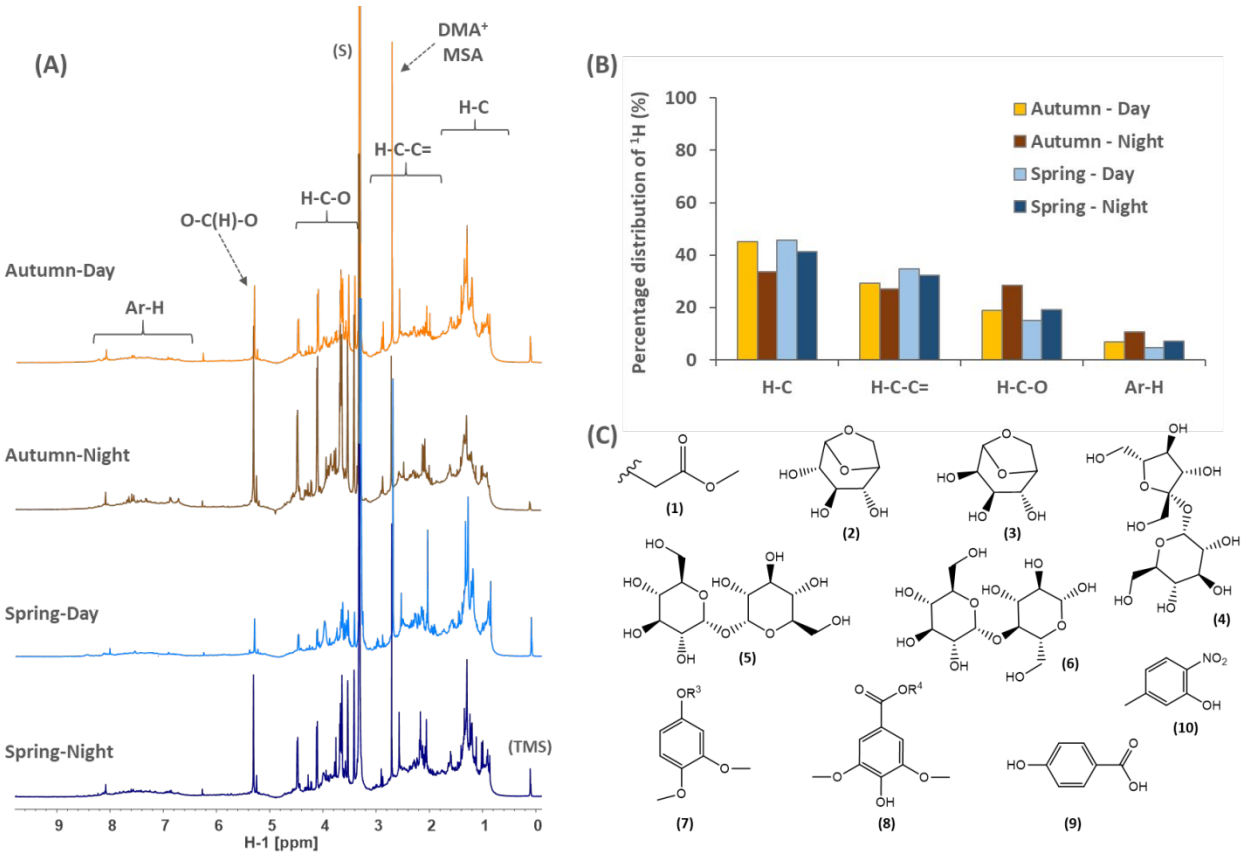

730

731 **Figure 1.** (A) Liquid-state ^{1}H NMR spectra of aerosol WSOM samples representative of day and

732 nighttime conditions in Autumn and Spring seasons, (B) percentage distribution of ^{1}H NMR in

733 each aerosol WSOM sample, and (C) aliphatic, carbohydrate and aromatic substructures

734 identified in aerosol WSOM collected overnight in Autumn. See Figures S9 and S10 (in SI)

735 for spectral assignments and identity of aromatic substituents (R^3 and R^4). Four spectral

736 regions are identified in ^{1}H NMR spectra (A): H–C, H–C–C=, H–C–O, and Ar–H. NMR

737 resonances assigned to dimethylammonium (DMA^+), methanesulfonic acid (MSA), and

738 protons bound to anomeric carbons [O–C(H)–O] are also identified. Additional resonance

739 signals: solvent (S) – MeOH-d_4, and tetramethylsilane (TMS) – 0.03% (v/v).

740

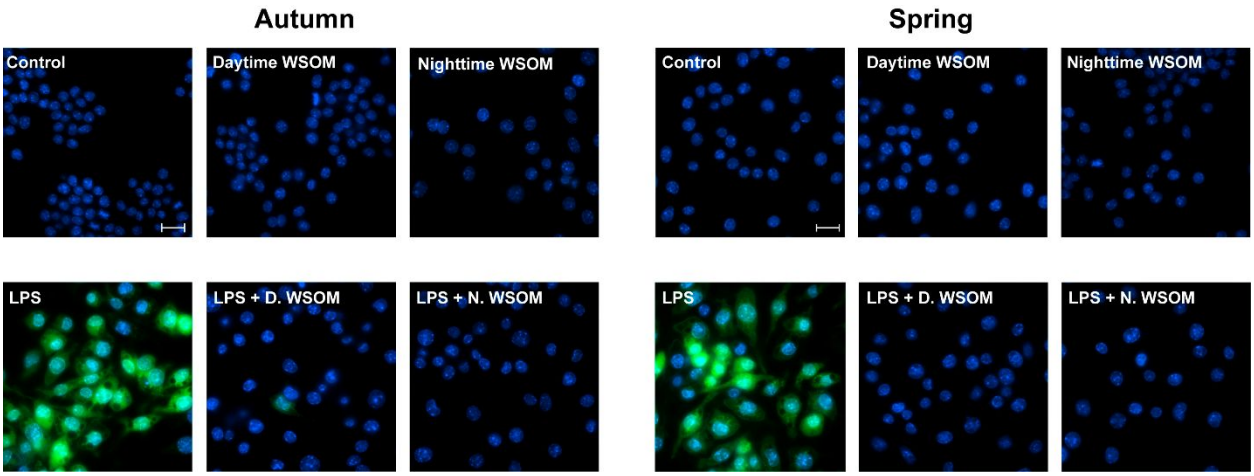

741

742 **Figure 2.** Effect of aerosol WSOM samples on macrophage ROS production and modulation of
743 LPS-induced oxidative stress. Cells were cultured in the indicated conditions and the ROS
744 production was assessed with H_2DCFDA (green), a ROS-sensitive fluorescent probe. Hoechst
745 (blue) was used to label the nuclei. Images representative of different fields were acquired at a
746 magnification of 63x (scale bar = 20 μm).

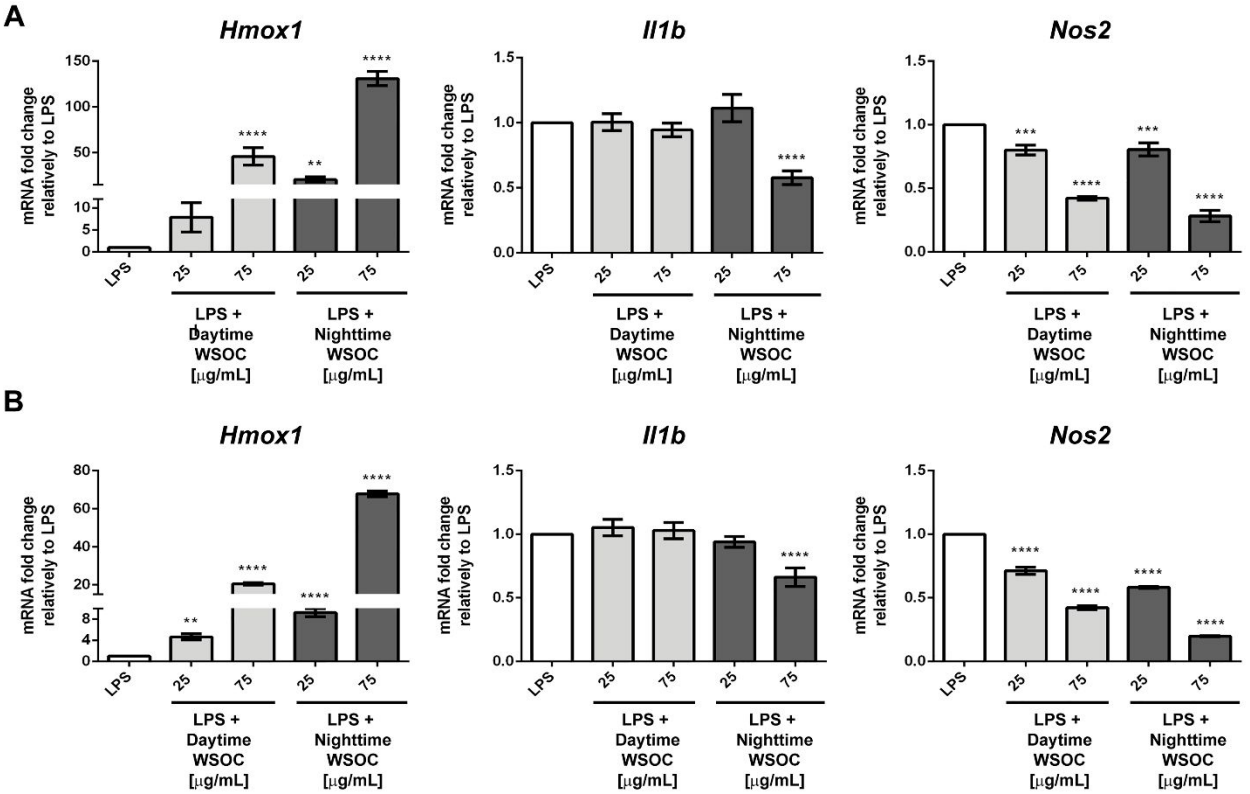

Figure 3. Effects of aerosol WSOM samples over LPS-induced transcription of *Hmox1*, *Il1b* and *Nos2* genes. Cells were exposed to different WSOC concentrations of (A) Autumn (A) and (B) Spring WSOC samples and then stimulated with LPS, followed by mRNA extraction and gene transcription assessment by q-PCR. Data is presented as mRNA fold change relatively to LPS-treated cells and represent the mean ± SD from at least 3 independent experiments. (*p<0.05; **p<0.01; ***p<0.001; ****p <0.0001: LPS *vs* WSOM+ LPS).

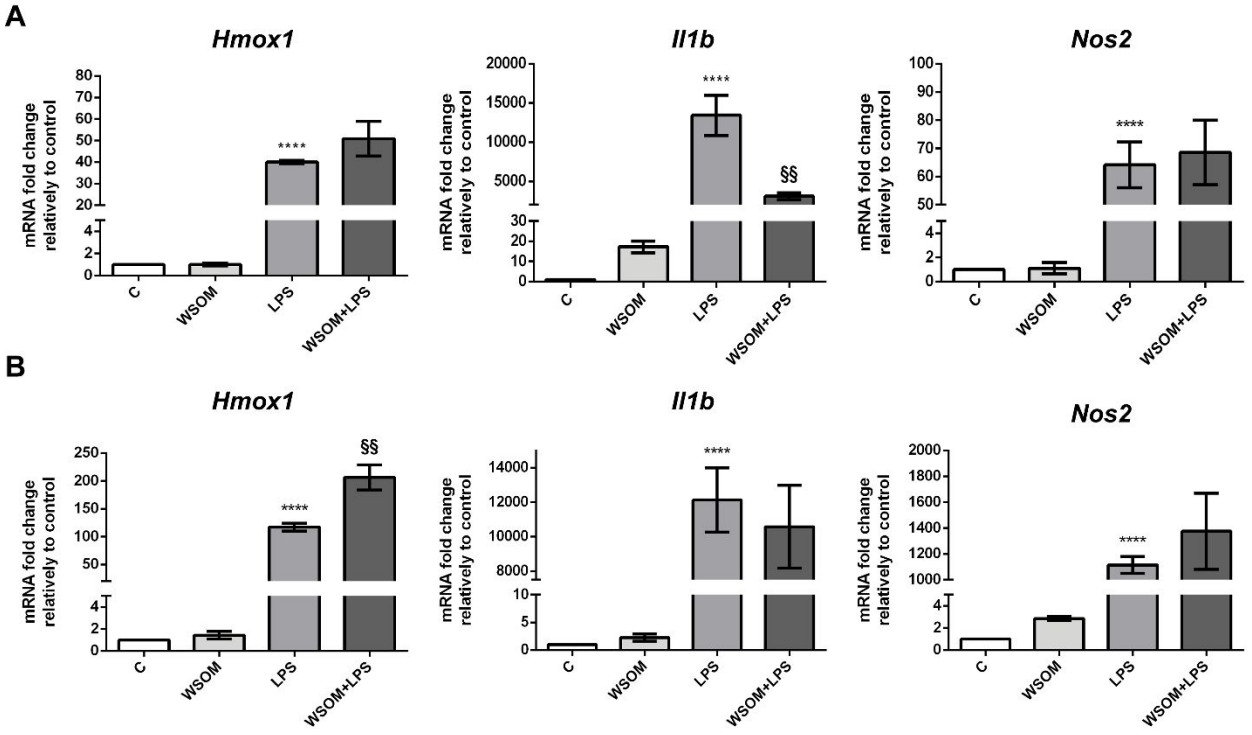

Figure 4. Impact of prolonged exposure to maximal theoretical doses of aerosol WSOM samples in the (A) gene transcription and (B) LPS-induced gene transcription of *Hmox1*, *Il1b*, and *Nos2*. Cells were exposed for 3 weeks to maximal theoretical quantities of WSOC extracts, followed by mRNA extraction and gene transcription assessment by q-PCR. Data is presented as mRNA fold change relatively to control or to LPS-treated cells and represent the mean ± SD from at least 3 independent experiments. [****$p<0.0001$: Control (C) *vs* treatments; §§$p<0.01$: LPS *vs* WSOM+LPS].

766 **Table 1.** Ambient concentrations (maximum – minimum; median) of urban $PM_{2.5}$, OC,

767 EC, WSOC, and WSOC/OC in each sampling period.

Season	Sampling Period	$PM_{2.5}$ ($\mu g\ m^{-3}$)	OC ($\mu g\ C\ m^{-3}$)	EC ($\mu g\ C\ m^{-3}$)	WSOC ($\mu g\ C\ m^{-3}$)	WSOC/OC (%)
Autumn	Day	60 – 14; 32	14 – 1.6; 4.1	2.2 – 0.3; 1.3	5.6 – 0.2; 1.3	39 – 12; 34
	Night	75 – 10; 47	20 – 1.5; 14	5.0 – 0.3; 3.0	6.5 – 0.5; 4.7	34 – 29; 33
Spring	Day	30 – 5.1; 21	6.2 – 0.75; 3.3	1.2 – 0.0; 0.4	2.7 – 0.43; 1.1	57 – 32; 42
	Night	29 – 3.2; 22	6.3 – 1.3; 4.3	1.4 – 0.3; 0.9	2.6 – 0.54; 1.6	44 – 35; 41

768

769

770

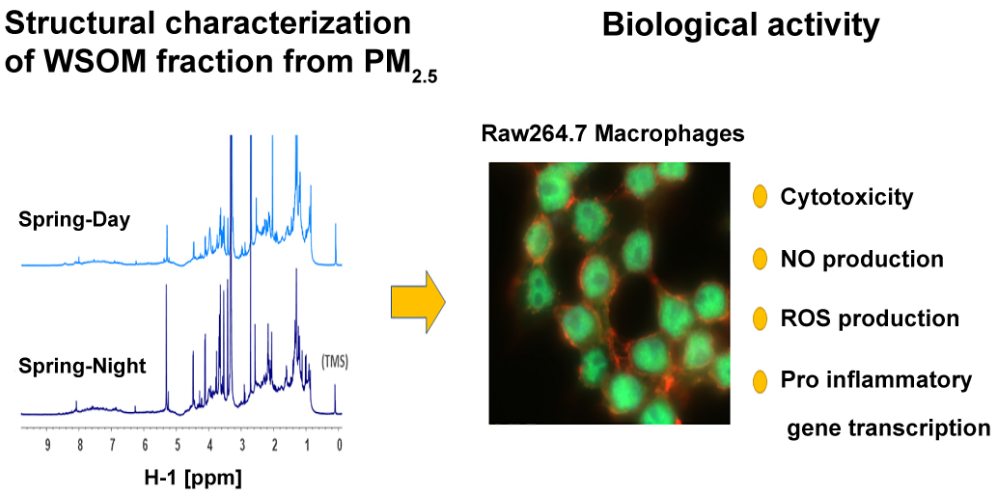
Structural characterization of WSOM fraction from PM2.5
Biological activity
Spring-Day
Spring-Night
(TMS)
9 8 7 6 5 4 3 2 1 0
H-1 [ppm]
Raw264.7 Macrophages
Cytotoxicity
NO production
ROS production
Pro inflammatory gene transcription

TOC Art